Extended Abstracts of the 21st Conference on Solid State Devices and Materials, Tokyo, 1989, pp. 297-300

D-4-3

Two-Valley Transport Equation Approach for AlGaAs/GaAs HBTs

Kazutaka Tomizawa and Dimitris Pavlidis†

Meiji University, School of Engineering
1-1-1 Higashimita Tamaku Kawasaki Japan

Transport equations for particle, momentum and energy densities in two conduction bands are applied to a self-consistent numerical simulation of heterojunction bipolar transistors. Simple formulas for the relaxation frequencies are proposed, by which the variation of the conduction band energy and doping concentration in a heterostructure device are easily taken into account. The electron transport in the AlGaAs/GaAs heterojunction bipolar transistor with two different collector structures is analyzed and discussed.

1. Introduction

We present in this paper a novel HBT model in which the electron transport equations for particle, momentum and energy densities in two conduction bands are employed. The collision terms in the transport equations are approximated by the relaxation times which are functions of electron energy. The relaxation times are expressed by simple interpolation formulas whose parameters can be modified in conformity with the variation of the band structure and doping concentration in a heterostructure device. The devices simulated are AlGaAs/GaAs HBT's with a wide-gap emitter, a graded-gap base and two different structures for collector space-charge region (SCR).

2. Simulation Method

The conservation equations for particles, momentum and energy are employed in order to describe the electron motion. We employed a similar relaxation time approximation proposed by Stewart et al.[1] as follows :

$$\left(\frac{\partial n_i}{\partial t}\right)_c = -n_i f_{nij}(w_i) + n_j f_{nji}(w_j) \tag{1}$$

$$\left(\frac{\partial p_i}{\partial t}\right)_c = -p_i f_{pi}(w_i) - p_i f_{nij}(w_i) \tag{2}$$

$$\left(\frac{\partial w_1}{\partial t}\right)_c = -(w_1 - w_0) f_{w1}(w_1) + \frac{w_{12}(w_1)}{n_1}\left(\frac{\partial n_1}{\partial t}\right)_c \tag{3}$$

$$\left(\frac{\partial w_2}{\partial t}\right)_c = -(w_2 - w_0) f_{w2}(w_2) \tag{4}$$

where i is the index of the conduction bands (i=1 for Γ-valley and i=2 for L-valleys). n_i is the electron density, p_i is the mean momentum density, and w_i is the mean energy density per electron. f_{nij} and f_{nji} are the relaxation frequencies which are related to the variation of electron density due to the intervalley transfer. f_{pi} is the momentum relaxation frequency, and f_{w1} and f_{w2} are the energy relaxation frequencies. w_{12} is the average transfer energy when electrons are transferred from the Γ-valley to the L-valleys. w_0 is the background energy density associated with the lattice temperature.

The various relaxation frequencies and

† Department of EECS, University of Michigan
1301 Beal Avenue, Ann Arbor, MI48109, USA.

w_{12} employed in Eqs.(1)-(4) are functions of electron energy w_1 or w_2. These are numerically obtained by a Monte Carlo simulation by considering a uniform electric field applied across the material under study and are expressed by simple interpolation formulas presented in Table 1.

The critical energy w_c which is employed in the interpolation formulas corresponds to the energy separation between the Γ- and L-valleys. w_c varies consequently with material composition.

The numerical calculation regarding the transport equations for electrons and the continuity equation for holes were made self-consistently with Poisson equation.

3. Results and Discussion

The two HBT structures simulated are shown in Fig.1. The collector SCR is different in the two devices corresponding to conventional HBT (HBT_{conv}) and inverted-field HBT (HBT_{invt}). The base is linearly graded with an Al fraction x=0.1 at the emitter-base junction and x=0.0 at the base-collector junction.

Fig.2(a),(b) shows the carrier density profiles in HBT_{conv} and HBT_{invt}. The solid curves n_1 and n_2 show the electron densities in the Γ- and L- valleys, respectively, while the dotted curves show the hole density. It is seen that the density of Γ-valley electrons is higher than that of the L-valley electrons in the emitter and base regions because the bottom of the L-valleys is located higher energy than the bottom of the Γ-valley. This changes, however, in HBT_{conv} towards to the base-collector junction, where the high electric field causes intervalley transfer. On the contrary the L-valley electrons in HBT_{invt} do not increase steeply near the base-collector junction but show a smooth Γ to L transition somewhere between the base and n^+ collector. This is due to the inverted-field profile, where the field becomes very high closer to the n^+ collector.

Fig.3 shows the corresponding profiles of the average electron velocity in the HBT_{conv} (solid curve) and the HBT_{invt} (dotted curve) at the bias condition. It is seen that the

$$f_{n12} = \frac{3w_1^2 + 6.2(w_1 - w_c + 0.33)(w_1/w_c)^6}{1 + (w_1/w_c)^6} \times 10^{13}$$

$$f_{n21} = (1.5 + 1.2w_2) \times 10^{12}$$

$$f_{p1} = \frac{C_{imp} + 2.9 + 170(w_1 + w_0)(w_1/w_c)^6}{1 + (w_1/w_c)^6} \times 10^{12}$$

$$f_{p2} = 8 \times 10^{13}\sqrt{w_2}$$

$$f_{w1} = \frac{0.4 + 2.8(w_1/w_c)^8}{(w_1 + 0.2)\left[1 + (w_1/w_c)^8\right]} \times 10^{12}$$

$$f_{w2} = \frac{1.2}{\sqrt{w_2}} \times 10^{12}$$

$$w_{12} = \frac{w_0 + w_c + 1.4(w_1 + w_0)(w_1/w_c)^6}{1 + (w_1/w_c)^6}$$

$$C_{imp} = 1.6\left(\frac{N_I}{10^{19}}\right)^{0.4} \times 10^{13}$$

Table.1 The interpolation formulas for various relaxation frequencies f's and w_{12}, where w_c (=0.33-0.75x) is the critical energy for the intervalley transfer, and N_I is the impurity concentration.

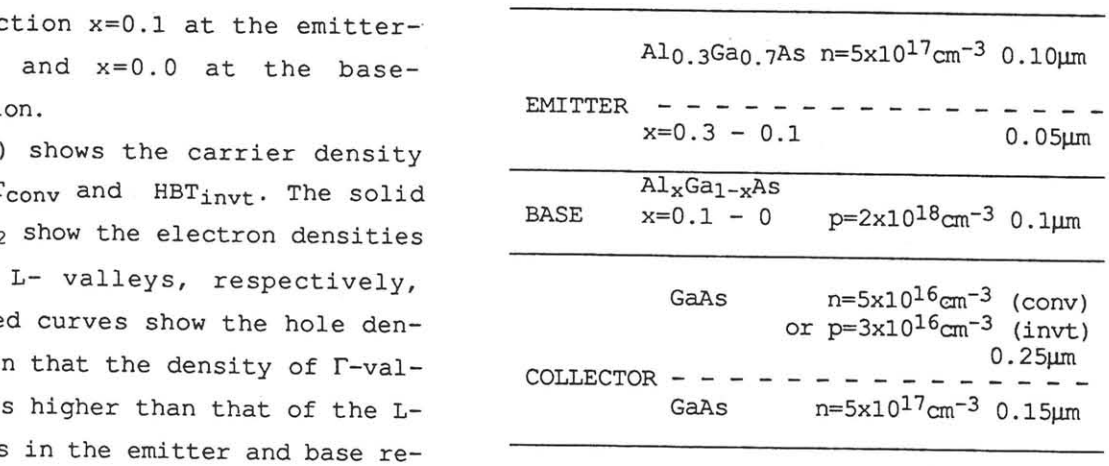

Fig.1 AlGaAs HBT model

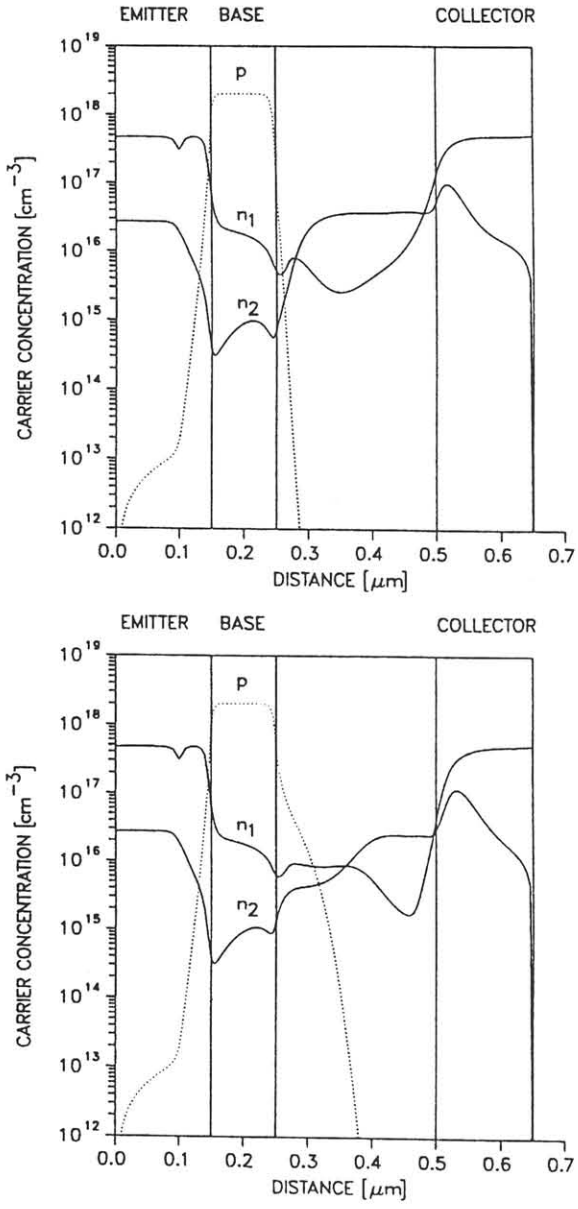

Fig.2 The carrier density profiles in HBT_{conv} (a) and HBT_{invt} (b). The solid curves n_1 and n_2 show the electron densities in the Γ- and L- valleys, respectively. The dotted curves show the hole density. V_{CE}=1.5V and V_{be}=1.37V.

average electron velocity < v > increases rather steeply in the base region because electrons are accelerated by the built-in electric field. < v > reaches a value, as high as 2 x 10^7 cm/s within a short distance from the emitter-base junction. The velocity is larger by a factor of 2 than our previous results obtained by Monte Carlo HBT simulation for identical designs[2]. This difference may be caused by the fact that the pre-

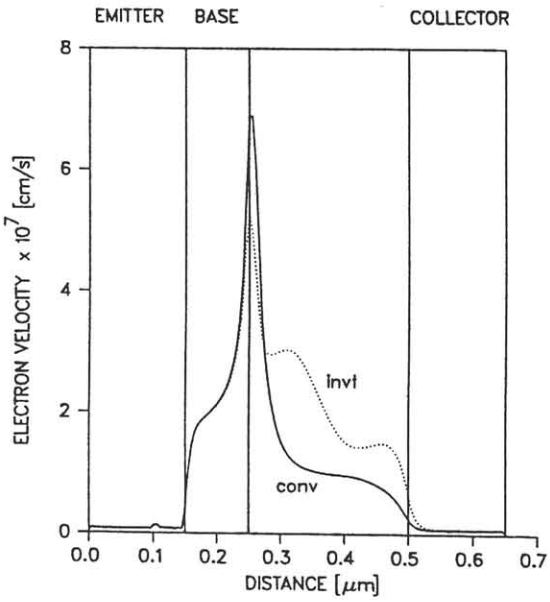

Fig.3 The profiles of the average electron velocity in the HBT_{conv} (solid curve) and the HBT_{invt} (dotted curve).

sent model does not take into account the effect of hole-plasmon scattering which was taken into account in the Monte Carlo HBT simulation.

A higher peak value of < v > is observed in the HBT_{conv}. This is caused by the fact that electrons injected into the SCR are accelerated more steeply by the higher electric field near the base-collector junction. However, the velocity overshoot in the SCR of the HBT_{conv} reached only within a distance of 500Å from the base-collector junction, because intervalley transfer takes place soon after the carrier injection into the SCR. The value of < v > is reduced afterwards to about 1 x 10^7 cm/s in the remaining SCR part of the HBT_{conv}.

The range of the velocity overshoot in case of the HBT_{invt} is longer than for HBT_{conv}. This is due to a gradual increase of the electric field in the SCR, which permits electrons to propagate over longer distance in the Γ-valley before intervalley transfer takes place. < v > remains as high as 3 x 10^7 cm/s at quite a distance from the base-collector junction. The distance and the amount

of the velocity overshoot observed in the present simulation are quite similar to those observed in the previous Monte Carlo simulation[2].

The unity-current-gain cut-off frequency f_T is calculated from the current density (I_C) over hole charge (Q_h) derivative. The f_T of HBT_{conv} and HBT_{invt} calculated in this way are shown by the solid curves in Fig.4. The collector bias is V_{CE} = 1.5V. f_T's calculated by the Monte Carlo method are also shown by the dotted curves in the same figure. The Monte Carlo program used accounts for hole-plasmon scattering. The presence of this scattering mechanism results in f_T values

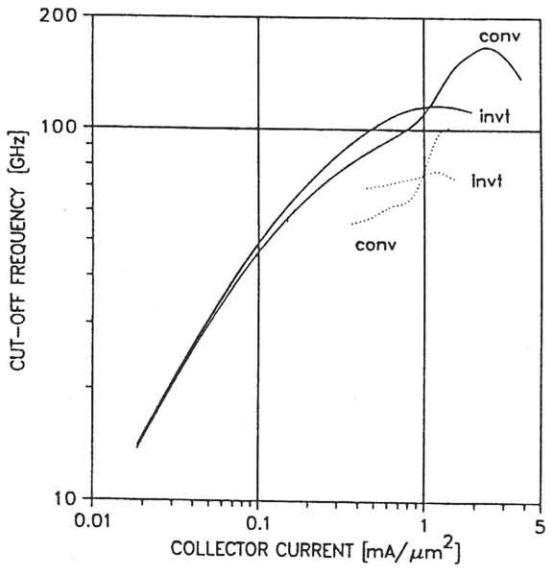

Fig.4 The unity-current-gain cut-off frequency f_T for HBT_{conv} (solid curve) and for HBT_{invt} (dotted curve). V_{CE}=1.5V.

which are lower by a factor of about 0.7 than those obtained by the transport equation method. However the behavior of f_T's as function of I_C are qualitatively same.

As shown in this section, the electron transport in HBT's and the values of f_T predicted in the presented model correlate well with those obtained by Monte Carlo simulation.

4. Conclusion

The transport equations for particles, momentum and energy densities in two conduction bands are applied to a self-consistent analysis of AlGaAs/GaAs HBT's, where useful formulas for the relaxation frequencies are employed by which the variation of the conduction band energy and doping concentration in a heterostructure device are easily taken into account.

The electron transport and device performance predicted by the present approach is quite similar to the one predicted by Monte Carlo simualtion, suggesting the usefulness of the present approach.

References

[1] R.A.Stewart et al.; Solid-State Electronics to be published.

[2] J.Hu, K.Tomizawa, and D.Pavlidis; IEEE. Electron Device Lett.(1989) 55.

Acknowledgement

The authors acknowledge the computing support of the CAEN at the University of Michigan. One of the author (K.T.) acknowledges the financial support of Meiji University for his sabbatical leave.